Position–specific contribution of interface tryptophans on membrane protein energetics

Deepti Chaturvedi[1] and Radhakrishnan Mahalakshmi[1,*]

[1]Molecular Biophysics Laboratory, Department of Biological Sciences, Indian Institute of Science Education and Research, Bhopal – 462066. India.

*To whom correspondence should be addressed: maha@iiserb.ac.in (R.M.)

SUPPORTING INFORMATION

EXPERIMENTAL SECTION

Protein expression, purification, and folding: Wild type OmpX (mature sequence of OmpX without the signal peptide) and its various mutants were expressed as inclusion bodies in *E. coli* C41 cells (www.overexpress.com) [1]. Inclusion bodies were dissolved in 8 M urea and purified by anion exchange chromatography on a HiPrep QFF column (GE Healthcare Lifesciences, Uppsala, Sweden). All purified proteins were folded in 50 mM DPC (n-dodecyl phosphocholine) prepared in 50 mM Tris-HCl pH 9.5, by rapid 20-fold dilution of the unfolded protein in 8 M urea into the folding mix, at 4 °C. A 3-minute heat shock was administered at 70 °C to promote complete folding of the protein [1], and preparation of the folded protein stock. The folded protein stock contained 150 μM OmpX, 50 mM DPC, 50 mM Tris-HCl pH 9.5 and 400 mM urea. Folded protein stocks were diluted 5-fold to 30 μM protein and 10 mM DPC for further experiments.

Equilibrium (un)folding monitored using fluorescence and circular dichroism: Equilibrium folding and unfolding measurements were monitored by recording the change in tryptophan fluorescence at 25 °C on a SpectraMax M5 microplate reader (Molecular Devices, LLC). The folded protein stock was unfolded by 5-fold dilution of the sample in various urea concentrations from 0.08 M – 9.5 M at 0.2 M increments. Similarly, the unfolded protein stock was diluted 5-fold in 9.5 M – 1.6 M urea, to promote folding. An excitation wavelength of 295 nm was used to collect emission spectra between 320-400 nm, at every 24 h, till 216 h using reported parameters [2, 3]. The system attained equilibrium at 216 h, and no further change in the fluorescence emission profiles was seen.

For fluorescence measurements, the average wavelength ($\langle\lambda\rangle$) was calculated using reported methods [4] at each urea concentration, using the fluorescence emission intensity recorded between 320-400 nm. Briefly, the average wavelength ($\langle\lambda\rangle$) is calculated as:

$$\langle\lambda\rangle = \Sigma(F_i\lambda_i) / \Sigma(F_i)$$

Here, λ_i is the i^{th} emission wavelength and F_i is the emission intensity at that wavelength. The absolute λ_{max} (wavelength at which maximum F_i is obtained) cannot be used as an observable to derive thermodynamic parameters, as this spectral property of tryptophan is not linearly proportional to the folded fraction [4]. Hence, the absolute λ_{max} cannot be fitted to a two state function, based on the linear extrapolation model. However, the $\langle\lambda\rangle$ becomes linearly proportional to the folded protein fraction when a correction factor (Q_R) is incorporated during the fit [4]. The use of $\langle\lambda\rangle$ also lowers variability introduced by pipetting viscous solutions such as lipids and detergents [5]. Hence, the $\langle\lambda\rangle$ value obtained at each urea concentration for each experiment was further fitted to a two state model after incorporation of Q_R, as described previously [4] and shown below:

$$y_O = \frac{(y_F + m_F[D]) + \frac{1}{Q_R}\,[(y_U + m_U[D])\exp[-(\Delta G^0_U + m[D])/RT]]}{1 + \frac{1}{Q_R}\exp[-(\Delta G^0_U + m[D])/RT]}$$

Here, ΔG^0_U is the equilibrium unfolding free energy, m is the unfolding cooperativity (or change in accessible surface area upon protein unfolding), y_O is the average wavelength at any denaturant concentration [D], R is the gas constant (1.987 cal K^{-1} mol^{-1}) and T is the temperature in kelvin. y_F and y_U are the $<\lambda>$ values of the folded and unfolded protein, respectively, while m_F and m_U are the slopes of the folded and unfolded baselines, respectively. Q_R is the correction factor, which is calculated as $Q_R = \Sigma(F_i)_{folded} / \Sigma(F_i)_{unfolded}$, where $(F_i)_{folded}$ is the fluorescence intensity of the folded protein at a specific wavelength, and $(F_i)_{unfolded}$ is the fluorescence intensity of the unfolded protein, for the same wavelength range used to derive $<\lambda>$; in our experiments, this is between 320-400 nm. The thermodynamic parameters thus derived include ΔG^0_U, m value, and C_m (midpoint of chemical denaturation). C_m was calculated by using the following equation: $C_m = \Delta G^0_U / m$. However, these thermodynamic parameters were not used further, as the folding/ unfolding transitions lacked a prominent post-transition baseline in many mutants, including WT.

For all OmpX variants including the mutants lacking tryptophan, far-UV circular dichroism (CD) wavelength scans were recorded between 205-260 nm at 25 °C on a Jasco J815 CD spectropolarimeter (Jasco Inc., Japan), using reported methods [3]. The data were averaged over three accumulations and corrected for buffer and detergent contributions. The CD spectra were converted to molar ellipticity (ME) values using reported methods [1], using the following formula:

$$\mathrm{ME} = \frac{\theta}{10 \text{ x c x l}}$$

Here ME is the molar ellipticity in deg cm^2 $dmol^{-1}$, θ is the observed ellipticity (mdeg), c is the molar concentration (mol/L) and l is the path length of the cuvette in cm.

For CD measurements, the ME value at 215 nm (ME_{215}) data derived from the wavelength scans at each urea concentration was normalized between 0 and 1 using the ME values of samples containing the lowest and highest urea concentrations, respectively. This was plotted against the respective urea concentrations for each mutant to obtain the fraction unfolded (f_U) at that urea concentration. f_U was calculated using the equation [6] provided below:

$$f_U = \frac{y_O - y_F}{y_U - y_F}$$

Here, y_O is the observed CD value in mdeg, y_F and y_U are the ellipticities of the folded and unfolded proteins at lowest and highest urea concentrations, respectively. Each dataset

obtained from the CD wavelength scans was fitted to the two state equation [4, 6] provided below:

$$y_O = \frac{(y_F + m_F[D]) + (y_U + m_U[D]) \exp[-(\Delta G_U^0 + m[D])/RT]}{1 + \exp[-(\Delta G_U^0 + m[D])/RT]}$$

Here y_O is the observed ellipticity at any denaturant concentration D. y_F and y_U, m_F and m_U are the intercepts and slopes of the folded and unfolded baselines. R is the gas constant (1.987 cal K^{-1} mol^{-1}) and T is the temperature in kelvin. The thermodynamic parameters (ΔG^0_U, C_m) were derived for each independent experiment using a global m value of –1.41 kcal mol^{-1} M^{-1}, and then averaged to obtain the mean and s. d.

Densitometry analysis: Aliquots from the post-equilibrium unfolding and folding samples were mixed with the gel loading dye. Unboiled samples were examined on 15% SDS-PAGE gels for anomalous mobility shift of the folded protein. Protein samples in 8 M urea and SDS-PAGE gel loading dye were boiled for 3 min at 100 °C; these samples served as the controls. Protein bands on the gel were quantified by densitometry using Multi Gauge v2.3 as reported earlier [1], and the fraction folded (f_F) was plotted against the corresponding urea concentration. The midpoint of chemical denaturation (C_m) was derived by fitting the plot to a sigmoidal function. The mean and s. d. were calculated from independent experiments.

Isothermal unfolding kinetics: OmpX samples folded in DPC were incubated at every 1 °C from 87 °C to 93 °C, and the unfolding kinetics (collapse of secondary structure) were monitored with time by measuring the change in ellipticity at 215 nm. The data were fitted to a single exponential function to derive the rate of unfolding (k_U). The Arrhenius plot for each protein was generated by plotting ln k_U against 1000/T, where T is the temperature in kelvin. Each plot was fitted to a linear function to derive the activation energy for unfolding (E_{act}) as slope = $-E_{act}$/R, where R is the gas constant [7]. E_{act} values obtained from independent experiments were averaged to obtain the mean and s. d. of the mean.

SUPPLEMENTARY FIGURES

A

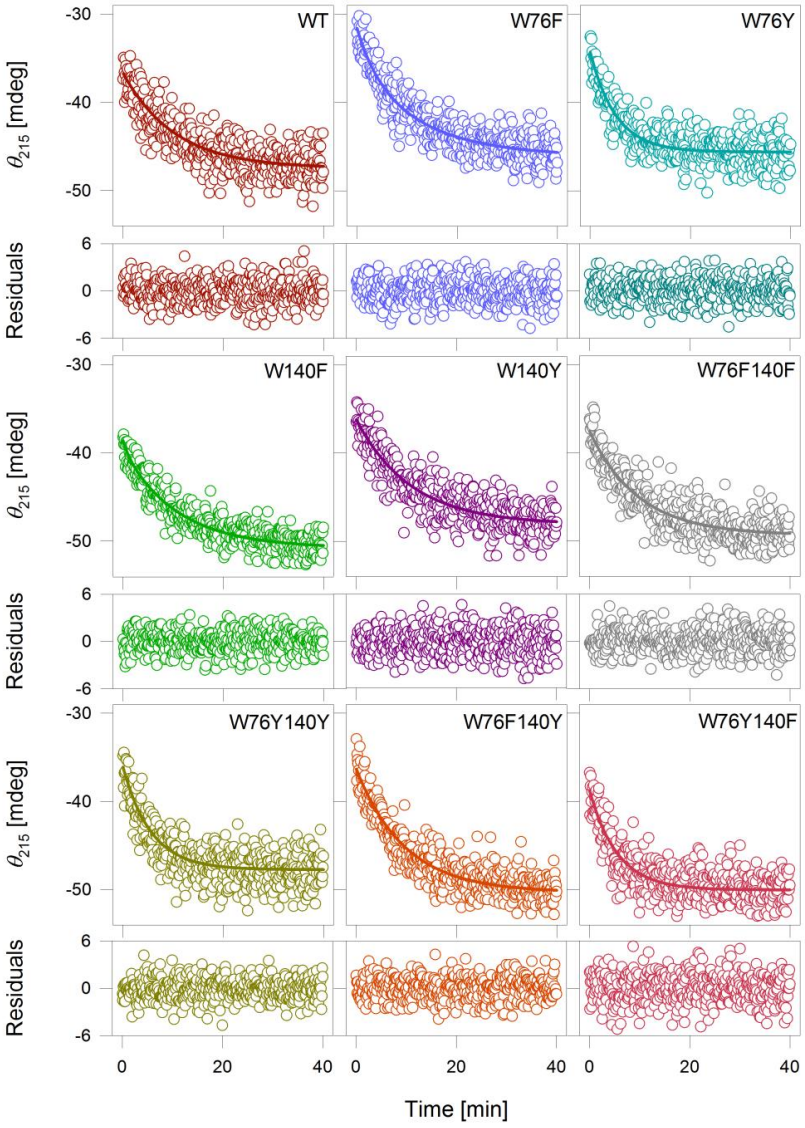

B

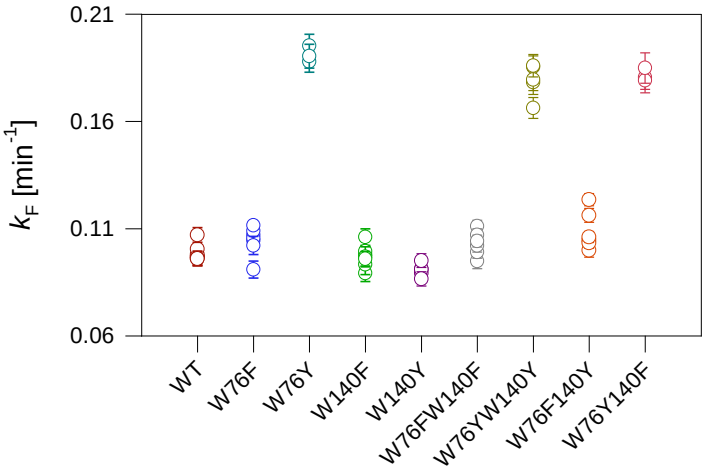

Figure S1. Contribution of positions 76 and 140 to OmpX folding rates in DPC micelles. The increase in ellipticity at 215 nm (θ_{215}) as OmpX folds at 25 °C is monitored using CD. Shown here in each plot as open circles, are the representative kinetic traces for each mutant. Folding was initiated by a 1:5 dilution of the unfolded protein in 8 M urea containing 50 mM DPC, with 50 mM Tris-HCl pH 9.5. The dead time of the experiment was ~15-20 s. Hence, residual structure was observed in all samples at the start of the recording. Folding was monitored for 40 min. (A) Shown here is the representative plot for each mutant from 0.017 min. Folding rates derived from fitting the ellipticity values (θ_{215}) to a single exponential function (fits are shown as solid lines). Below each kinetic trace is the panel showing residuals for the single exponential fit. Note that the data were fitted independently to derive the average folding rate and standard deviation (s. d.) summarized in Figure 2. The significance of the rates measured is shown in (B). Here, each point on the scatter plot denotes the rate obtained from fits of individual dataset to a single exponential function, with the error bars representing the goodness of fit. Data for each mutant is arbitrarily colored as: WT: maroon; W76F: blue; W76Y: teal; W140F: green; W140Y: purple; W76F140F: grey; W76Y140Y: olive; W76F140Y: orange; W76Y140F: dark pink.

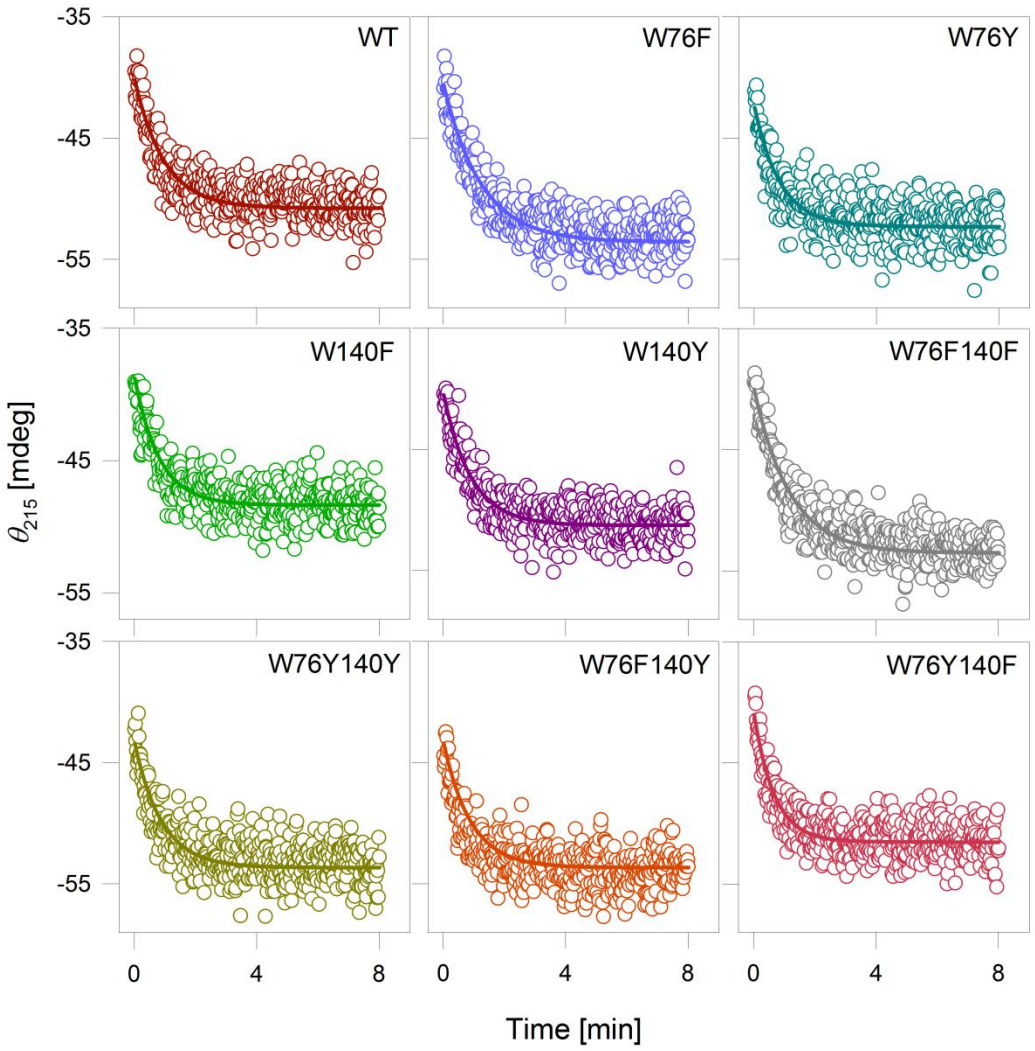

Figure S2a. OmpX folding kinetics in DMPC:DPC bicelles. Rate of folding in DMPC:DPC bicelles of q = 0.5, measured as an increase in ellipticity at 215 nm (θ_{215}), and shown as open circles in the plots above. Data was collected for up to 8 min. Shown here is the representative plot for each mutant from 0.017 min. Each kinetics trace is fitted to a single exponential function (solid lines) to derive the rate of folding. Note that the data from 3-5 such independent measurements were fitted independently to derive the average folding rate and s. d. summarized in Figure 2. Data for each mutant is arbitrarily colored as: WT: maroon; W76F: blue; W76Y: teal; W140F: green; W140Y: purple; W76F140F: grey; W76Y140Y: olive; W76F140Y: orange; W76Y140F: dark pink.

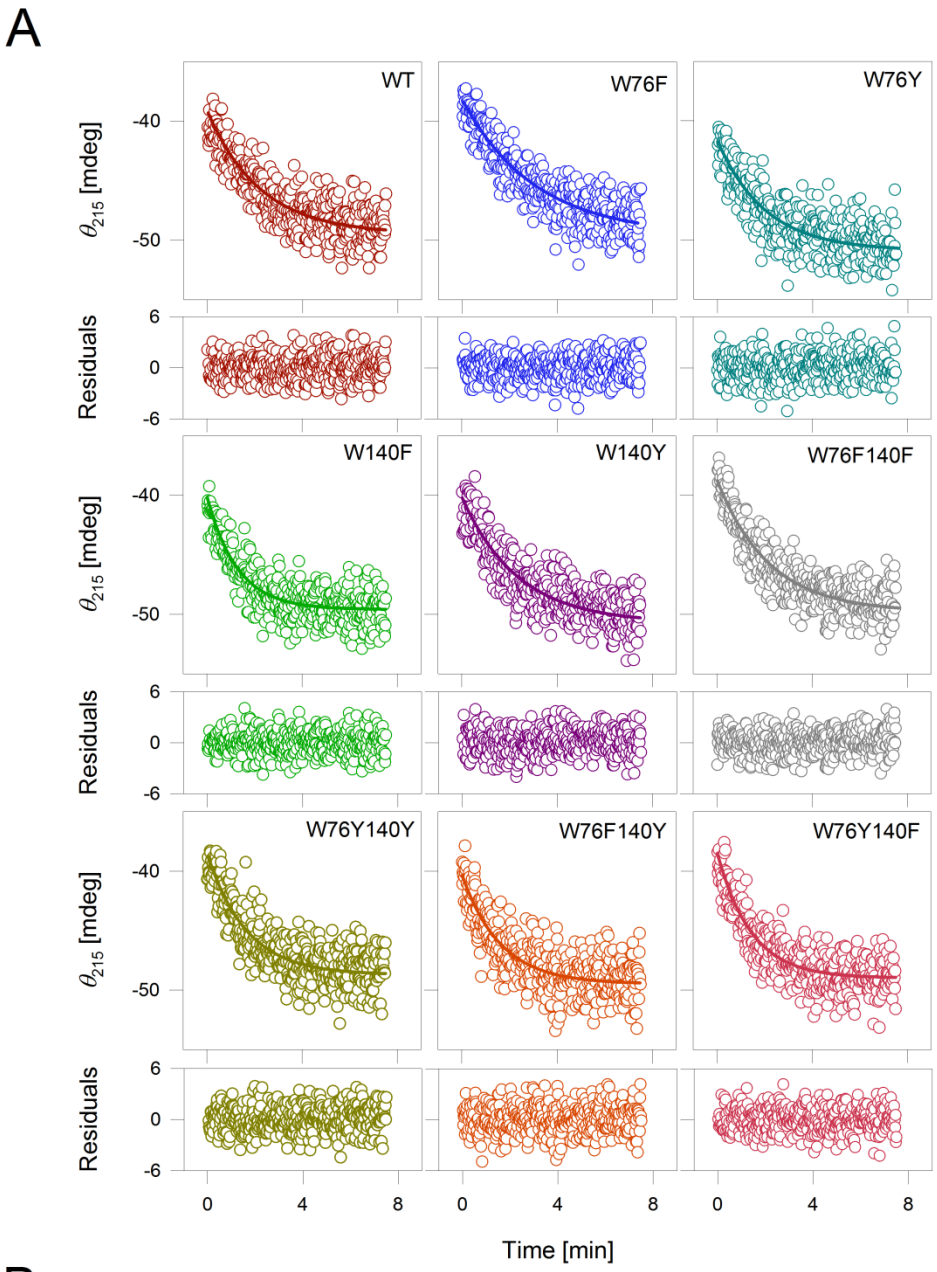
A
WT
W76F
W76Y
W140F
W140Y
W76F140F
W76Y140Y
W76F140Y
W76Y140F
θ_{215} [mdeg]
Residuals
Time [min]
B
k_F [min^{-1}]
WT
W76F
W76Y
W140F
W140Y
W76F140F
W76Y140Y
W76F140Y
W76Y140F

Figure S2b. Raw ellipticity profiles for OmpX folding kinetics in DMPC:DMPG:DPC bicelles. Representative kinetic traces of OmpX folding in DMPC:DPC bicelles doped with 20% DMPG, showing the rate of increase in θ_{215}. The rate of folding can be measured from the gain in secondary structure content with time, which is measured as an increase in θ_{215}. A bicelle q of 0.5 and a DMPC: DMPG ratio of 1:0.25 was maintained for all constructs. The dead time of the experiment was 15-20 s. Data was collected every 1 s for up to 8 min. (A) Shown here is the representative plot for each mutant from 0.017 min. The solid line in each plot represents the fit of the θ_{215} values to a single exponential function. Below each kinetic trace is the panel showing residuals of the single exponential fit of the respective plot. Note that the data from 3-5 such independent measurements were fitted independently to derive the average folding rate and s. d. summarized in Figure 2. The significance of the rates measured is shown in (B). Here, each point on the scatter plot denotes the rate obtained from fits of individual dataset to a single exponential function, with the error bars representing the goodness of fit. Data for each mutant is arbitrarily colored as: WT: maroon; W76F: blue; W76Y: teal; W140F: green; W140Y: purple; W76F140F: grey; W76Y140Y: olive; W76F140Y: orange; W76Y140F: dark pink.

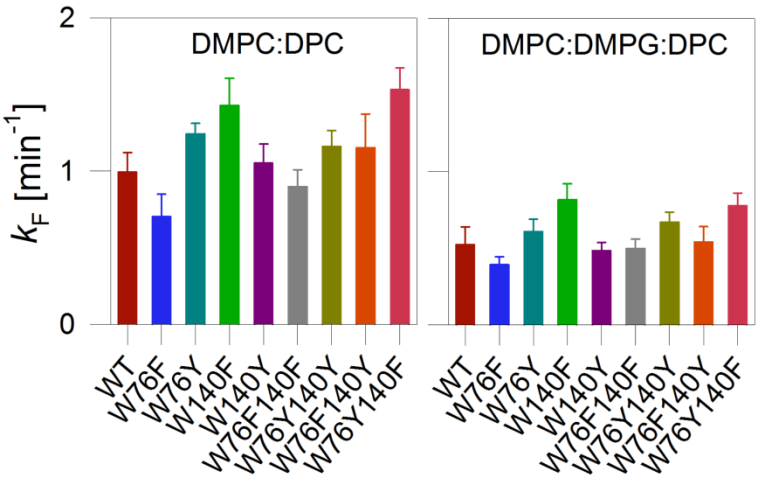

Figure S3. Folding kinetics of select OmpX mutants in bicelles. Shown above are the k_F values obtained in DMPC:DPC and DMPC:DMPG:DPC doped bicelles of q = 0.5. The values of k_F were obtained by fitting the folding profiles to a single exponential function. Errors represent s. d. obtained from 3-5 independent experiments. Data for each mutant is arbitrarily colored as: WT: maroon; W76F: blue; W76Y: teal; W140F: green; W140Y: purple; W76F140F: grey; W76Y140Y: olive; W76F140Y: orange; W76Y140F: dark pink.

Discussion on OmpX folding kinetics in bicelles

We find that the k_F of OmpX-WT (~1.0 min^{-1}) is 10–fold higher in bicelles than in micelles. This is a surprising result, as OMPs generally show slower folding rates in lipidic systems [8]. We find that lipidic systems can support fast folding of OmpX and its tryptophan mutants. While we have no clear explanation for this observation, we believe that the observed k_F may result from the use of isotropic bicelles. As seen in micelles (see Figure 2B), the folding rates of OmpX-W76Y and OmpX-W76Y140F is augmented also in bicelles. It is known that in the presence of phosphatidylglycerol (PG) lipids, the folding of OMPs is slower [9]. As expected, we obtained a 2.5–fold reduction in the k_F of OmpX in the doped bicelles. However, the measured k_F in doped bicelles remains ~2–fold higher than in DPC micelles. Here, the k_F of the OmpX mutants bearing Tyr76 is higher than OmpX-WT also in doped PC:PG bicelles. However, the magnitude of difference in k_F is lower. The k_F of W76Y is ~1.2–fold greater than WT, and that of W76Y140F is ~1.5–fold higher. Interestingly, Phe140 considerably augments the k_F of OmpX only in bicelles (>1.5–fold; compare the k_F of W140F mutant in Figure 2 and this figure). While we do not have a convincing explanation for this observation, we speculate that the hydrophobic nature of phenylalanine [10] might contribute to the enhanced folding rate of OmpX in lipidic bicelles. However, the folding rate of W76Y140F is only marginally higher than the respective single-Trp tryptophan mutants W76Y and W140F, indicating that under our experimental conditions, the effect of the mutations is non-additive.

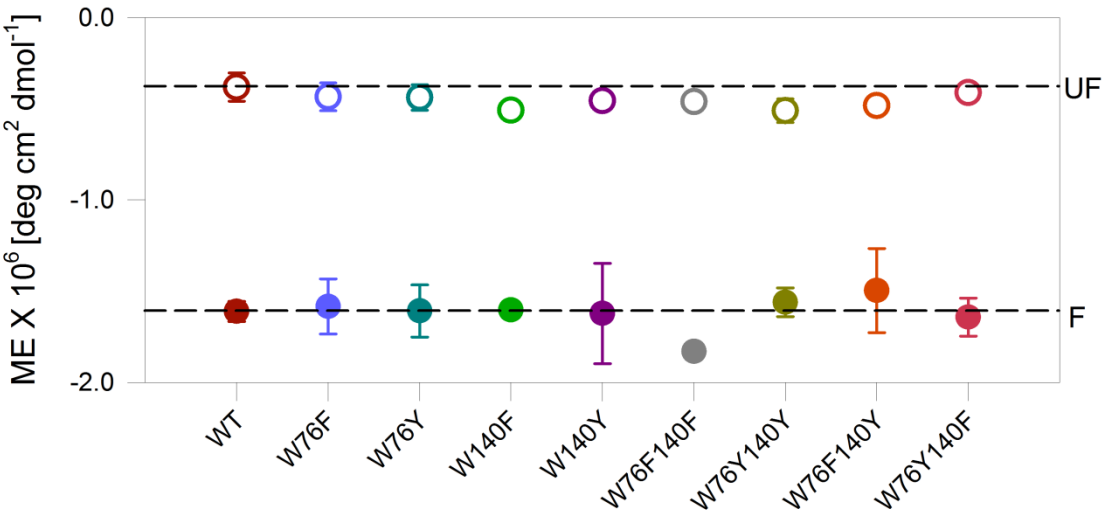

Figure S4. Secondary structure content of folded and unfolded forms of OmpX and its mutants. The molar ellipticity (ME) values reflecting the secondary structure content of OmpX and its mutants at 215 nm, are presented here at the lowest (folded, F) and highest (unfolded, UF) urea concentrations of 80 mM and 8 M, respectively. It is evident that all the mutants possess substantial and similar secondary structure content in their folded state. Also, all the mutants attain similar residual secondary structural content upon unfolding by urea. All values are obtained from post-equilibrium unfolding measurements at 216 h, using CD (OmpX does not aggregate under such prolonged incubations in urea (see Figure S5)). Hence, the loss in secondary structure content upon unfolding of OmpX, and within experimental limits, is likely to be independent of the mutation. Error bars denote s. d. of the mean, and are derived from independent experiments. Data for each mutant is arbitrarily colored as: WT: maroon; W76F: blue; W76Y: teal; W140F: green; W140Y: purple; W76F140F: grey; W76Y140Y: olive; W76F140Y: orange; W76Y140F: dark pink.

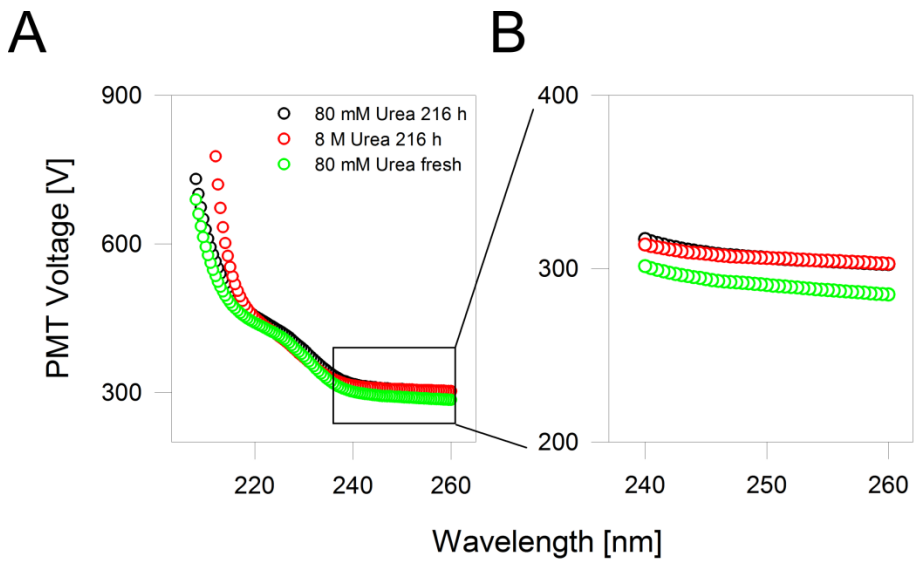

Figure S5. OmpX is not prone to aggregation upon prolonged incubation. (A) Left panel shows the change in photomultiplier tube (PMT) voltage during acquisition of the far-UV CD wavelength scans recorded from 207-260 nm for OmpX WT folded in DPC micelles. Absorption or scattering of the incident light by buffer components (<220 nm), protein aggregates or particulate matter (>240 nm) lowers the amount of light that is incident on the PMT (detector), correspondingly increasing the applied PMT voltage. Shown here are the PMT values measured for representative 216 h post-equilibrium OmpX WT in 80 mM (folded sample, black circles) and 8 M (unfolded sample, red circles) urea concentrations. Also overlaid is the change in PMT voltage for a freshly folded OmpX WT sample (green circles). Note how the change in PMT voltage between 240-260 nm (expanded in (B)) is negligible in all three samples, even after 216 h incubation at 25 °C, suggesting that OmpX does not aggregate upon incubation for 216 h. This is further confirmed by NMR spectra of samples recorded after incubation at 25 °C for 6-9 months [1].

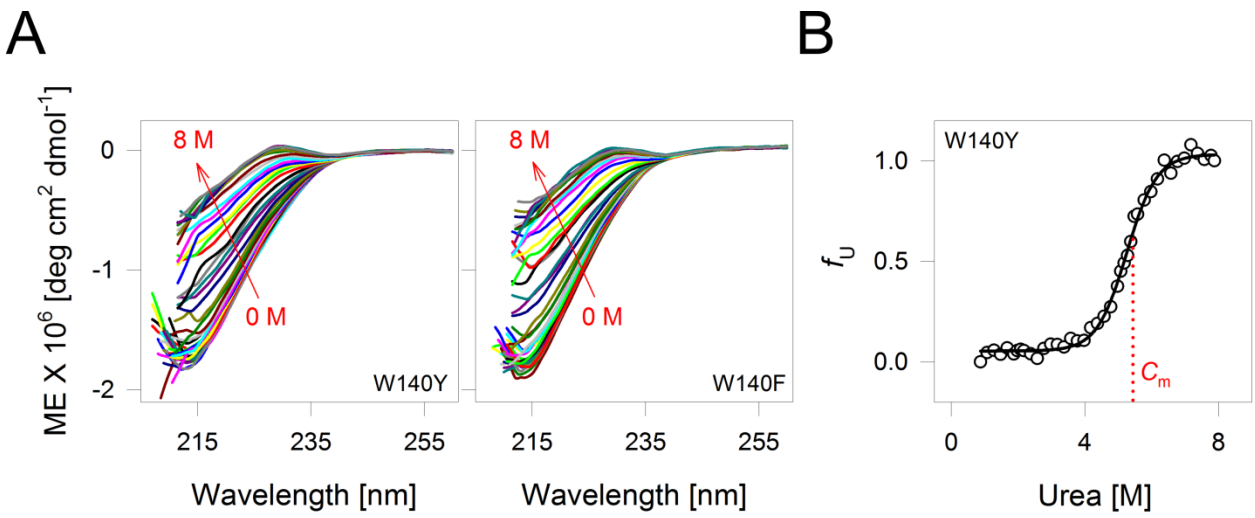

Figure S6. Thermodynamic studies from post-equilibrium structural measurements. (A) Far-UV CD wavelength scans were recorded for all the OmpX mutants folded in DPC micelles, after incubation in various urea concentrations for 216 h. Data were obtained at 25 °C from ~205 nm to 260 nm, and the fraction unfolded (f_U) at each urea concentration was derived, from CD values at 215 nm. Two representative raw datasets (CD wavelength scan corrected only for buffer contributions) for the W140Y (left) and W140F (right) mutant is shown here at various urea concentrations from 80 mM – 8.0 M urea. The data are presented as total molar ellipticity (ME) values, calculated using reported methods [1]. The ME value at 215 nm for the unfolding measurements was normalized between 0 and 1 to obtain the fraction unfolded (f_U) at each urea concentration. One such representative plot is shown in (B) for W140Y. The normalized data is fitted to a two-state function shown as solid black line in plot (B) to derive the ΔG^0_U and C_m. The definition of C_m is illustrated in (B) using the dotted red drop line. The f_U plots for all mutants are shown in Figure S7.

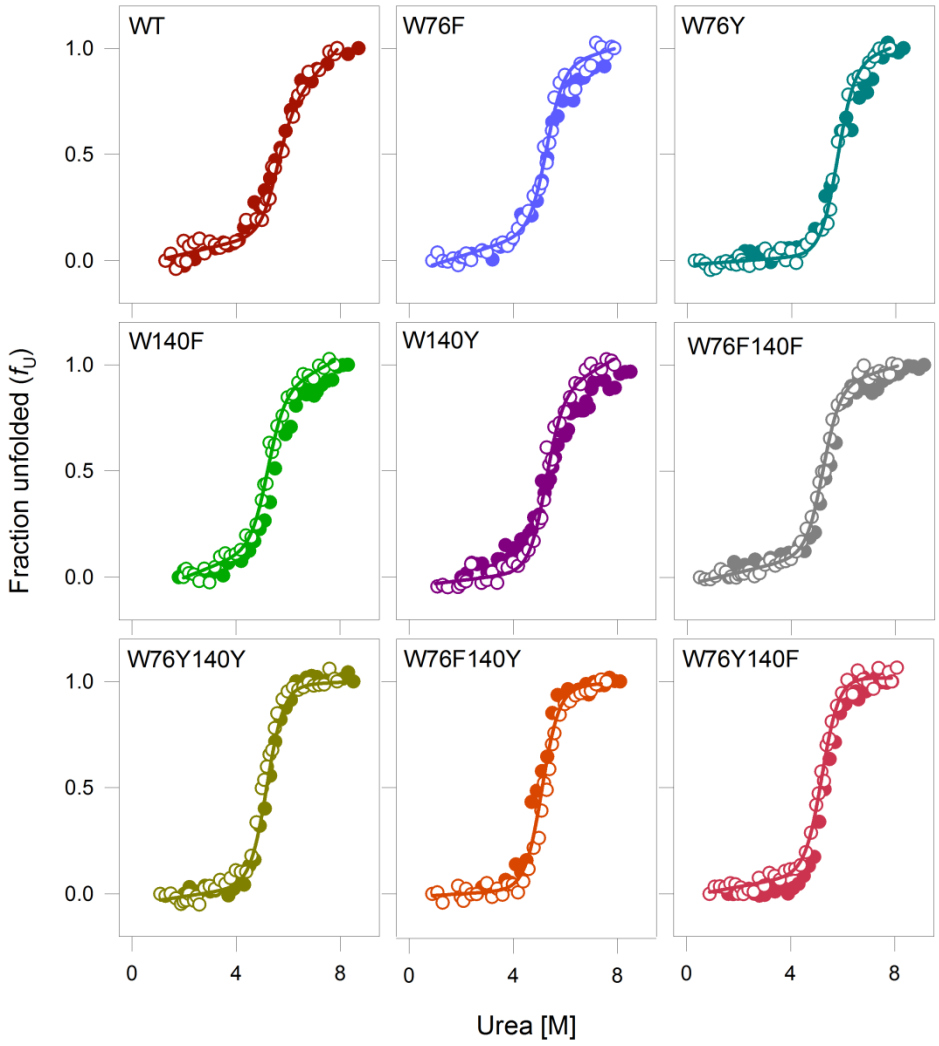

Figure S7. Equilibrium chemical denaturation measurements of OmpX mutants in DPC. The extent of urea-induced denaturation (monitored as the change in θ_{215}) is normalized between 0 and 1 and shown as fraction unfolded (f_U) plots. The open circles represent the equilibrium unfolding whereas filled circles represent the equilibrium folding measurements. Equilibrium was achieved at 216 h. OmpX does not aggregate under such prolonged incubations in urea (see Figure S5). Shown here are the representative folding and unfolding profiles for each mutant. Each far-UV CD profile was recorded post-equilibrium (see Figure S6A for a representative dataset). The CD value obtained at 215 nm for each denaturant concentration was normalized between 0 and 1, and fitted to a two-state unfolding model with a global *m* value of –1.41 kcal mol^{-1} M^{-1} (for purpose of clarity, only fits for the unfolding profile are shown as solid lines). Note that within limits of experimental error, the folding and unfolding profiles superimpose well. Overlap between the folding and unfolding profiles establishes path independence for all the mutants. Fits of the data obtained from the unfolding profile was used to derive the thermodynamic parameters (summarized in Figure 3). Data for each mutant is arbitrarily colored

as: WT: maroon; W76F: blue; W76Y: teal; W140F: green; W140Y: purple; W76F140F: grey; W76Y140Y: olive; W76F140Y: orange; W76Y140F: dark pink.

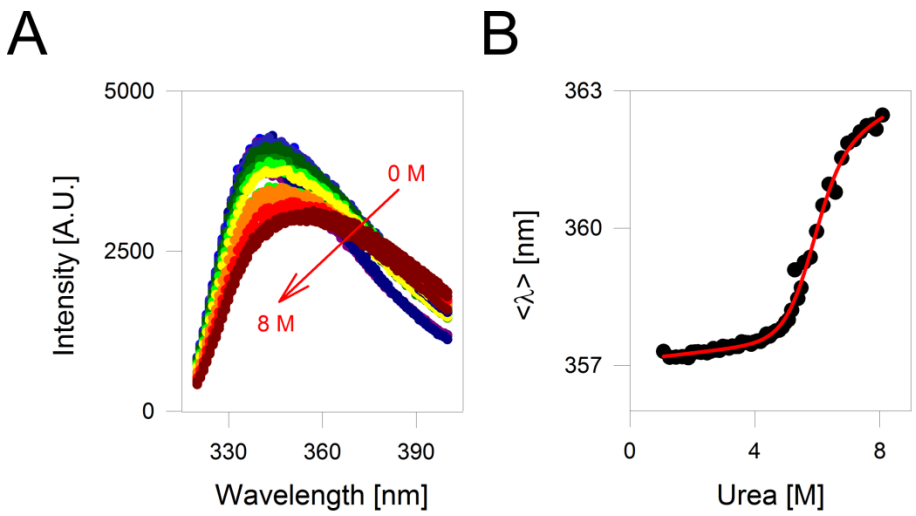

Figure S8. Representative fluorescence emission profile of OmpX WT. (A) Representative Trp fluorescence emission scans of OmpX WT folded in DPC micelles, and unfolded using increasing concentrations of urea from 80 mM to 8 M. The emission spectra at various concentrations of urea are represented as a gradient from dark blue (lowest urea) to dark red (highest urea). (B) The values of average wavelength (black filled circles) calculated at each urea concentration from the 216 h equilibrium unfolding fluorescence spectra of OmpX WT presented in (A). All the thermodynamic parameters were derived from fitting these average wavelength plots to a two state function (fit is shown as a solid red line in (B)). Data for all the mutants is summarized in Figure S9.

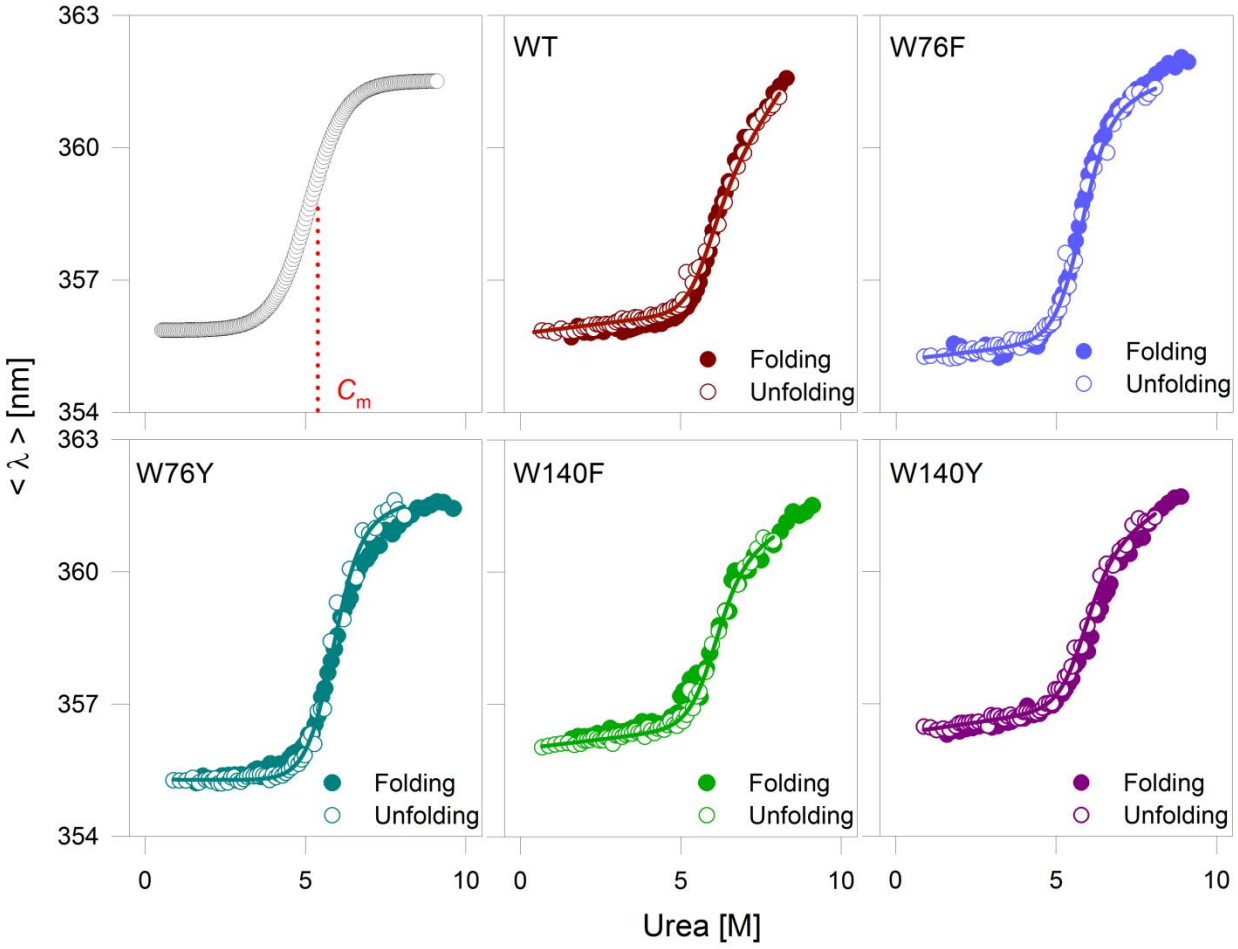

Figure S9. Comparison of folding and unfolding profiles derived by monitoring changes in Trp fluorescence. For the subset of OmpX mutants possessing at least one tryptophan, the change in the tryptophan fluorescence was monitored at 25 °C. The protein in DPC micelles was incubated in various concentrations of urea for up to 216 h. The average emission wavelength (<λ>) plots were calculated using previous reports [4], and are plotted here against the respective urea concentrations for the 216 h time point. Schematic representing an average wavelength plot highlighting the C_m (red dotted drop line) is shown in the top left panel. Shown in the other panels are the representative folding and unfolding equilibrium profiles for all the mutants. The filled circles represent the folding and the open circles represent the unfolding profiles. Note that within limits of experimental error, the folding and unfolding profiles superimpose well. Solid lines represent fits of the average wavelength plots to a two state function, and are shown only for the unfolding profile for purpose of clarity. Note that a few mutants including OmpX-WT lack a prominent post-transition baseline. Hence, the fits of the data obtained from fluorescence measurements are not very reliable. Note that the data obtained from CD measurements (Figure S7) monitors global changes in the secondary structure content, and show a more prominent post-transition baseline. Hence, data from CD are more reliable than that from fluorescence

measurements. Data for each mutant is arbitrarily colored as: WT: maroon; W76F: blue; W76Y: teal; W140F: green; W140Y: purple.

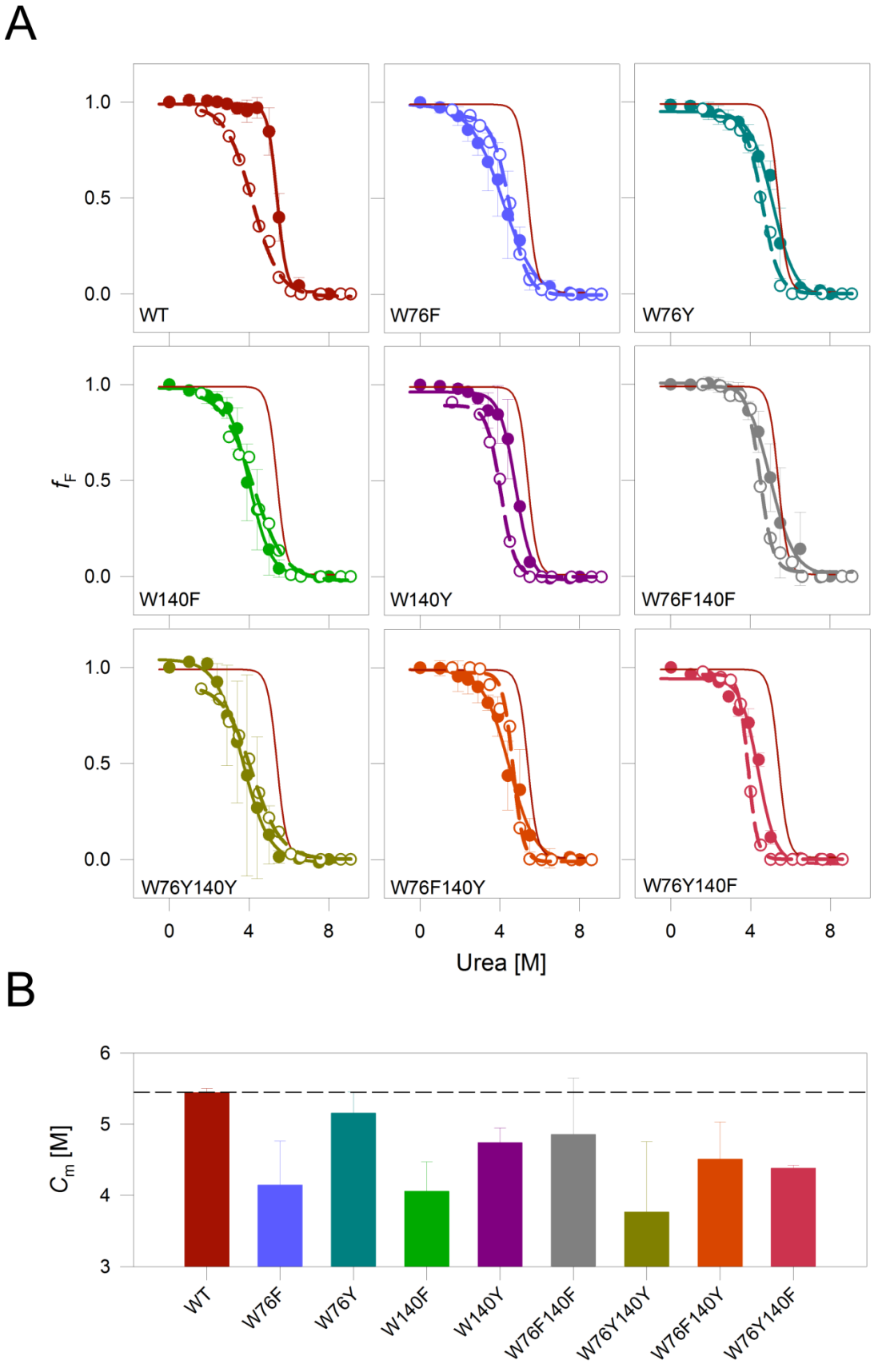
A
1.0
0.5
0.0
f_F
WT
W76F
W76Y
W140F
W140Y
W76F140F
W76Y140Y
W76F140Y
W76Y140F
0
4
8
Urea [M]
B
6
5
4
3
C_m [M]
WT
W76F
W76Y
W140F
W140Y
W76F140F
W76Y140Y
W76F140Y
W76Y140F

Figure S10. Densitometry analysis of gel mobility shifts in OmpX unfolding. OmpX shows a characteristic gel mobility shift when folded protein is analyzed on cold SDS-PAGE (SDS-PAGE gels run with unboiled samples) [1]. Here, we incubated OmpX and its mutant proteins folded in DPC micelles, at 25 °C for 216 h in various urea concentrations to unfold the protein. The samples were then mixed with the gel loading dye and loaded on 15% SDS-PAGE gels without boiling. The gel mobility shift seen for OmpX was quantified using densitometry by comparing the intensity of the folded monomer band with the combined intensity of the folded and unfolded bands [1]. The fraction folded (f_F) profiles thus derived from unfolding (filled circles) and folding (open circles), is plotted against the respective urea concentrations in (A) for the various mutants. The data were derived from 2-3 independent experiments and the mean values are shown here for representative concentrations of urea for the unfolding profiles. The profile for OmpX WT (dark red solid line) is included in every plot for comparison. The color scheme used here is: WT, dark red; W76F, blue; W76Y, cyan; W140F, green; W140Y, purple; W76F140F, grey; W76Y140Y, olive; W76F140Y, orange; W76Y140F, pink. The same color scheme is retained in (B). The data in panel A were fitted to a sigmoidal function (fits are shown as solid (unfolding) and dashed (folding) lines), to obtain the midpoint of chemical denaturation (C_m) for all the mutants. The C_m obtained from the unfolding profiles is plotted in (B). The C_m obtained for OmpX WT is shown as a black dashed line in (B). Data for each mutant is arbitrarily colored as: WT: maroon; W76F: blue; W76Y: teal; W140F: green; W140Y: purple; W76F140F: grey; W76Y140Y: olive; W76F140Y: orange; W76Y140F: dark pink. A comparison of the folding and unfolding profiles monitored using gel mobility shifts show the presence of hysteresis in nearly all the mutants. Hence, C_m derived from densitometry studies was not interpreted further.

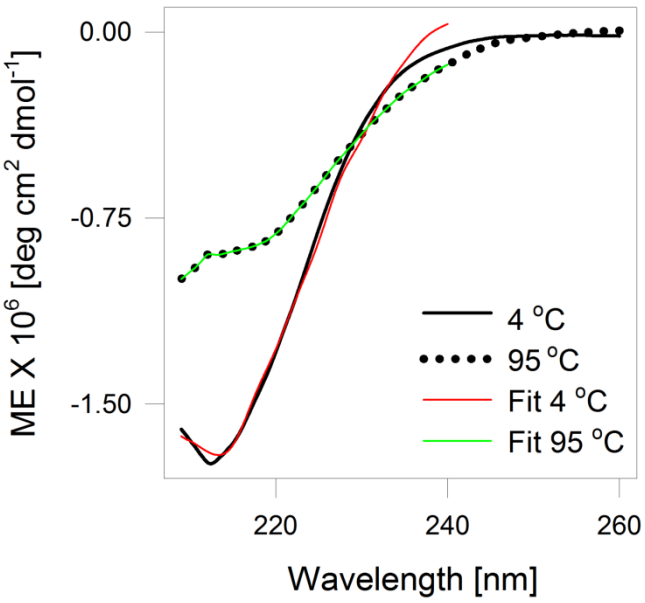

Figure S11. OmpX shows residual secondary structure content even upon unfolding by heating to 95 °C. Shown here is a representative far-UV CD wavelength scan of OmpX WT at 4 °C (black solid line) and 95 °C (black dotted line). The secondary structure content was estimated by fitting the data to the reference set of Reed and Reed [11]. Fits are shown as solid colored lines (red, 4 °C; green, 95 °C). The secondary structure content thus estimated for the unfolded protein was ~30-50% of the folded protein at 4 °C.

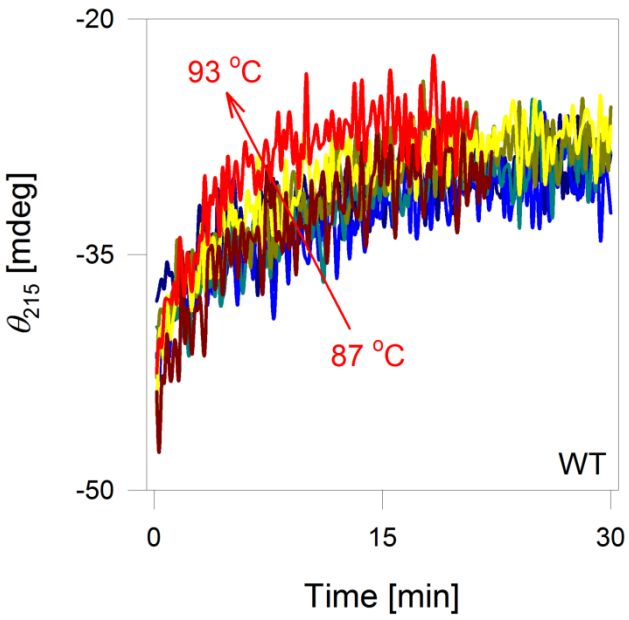

Figure S12. Isothermal unfolding measurements in DPC micelles. Representative unfolding profile of WT, monitored using change in θ_{215} (ellipticity at 215 nm) at a range of temperatures from 87 °C (dark blue) to 93 °C (dark red). Each unfolding isotherm was fitted to a single exponential decay function to derive unfolding rates, which were further used to estimate the activation energy.

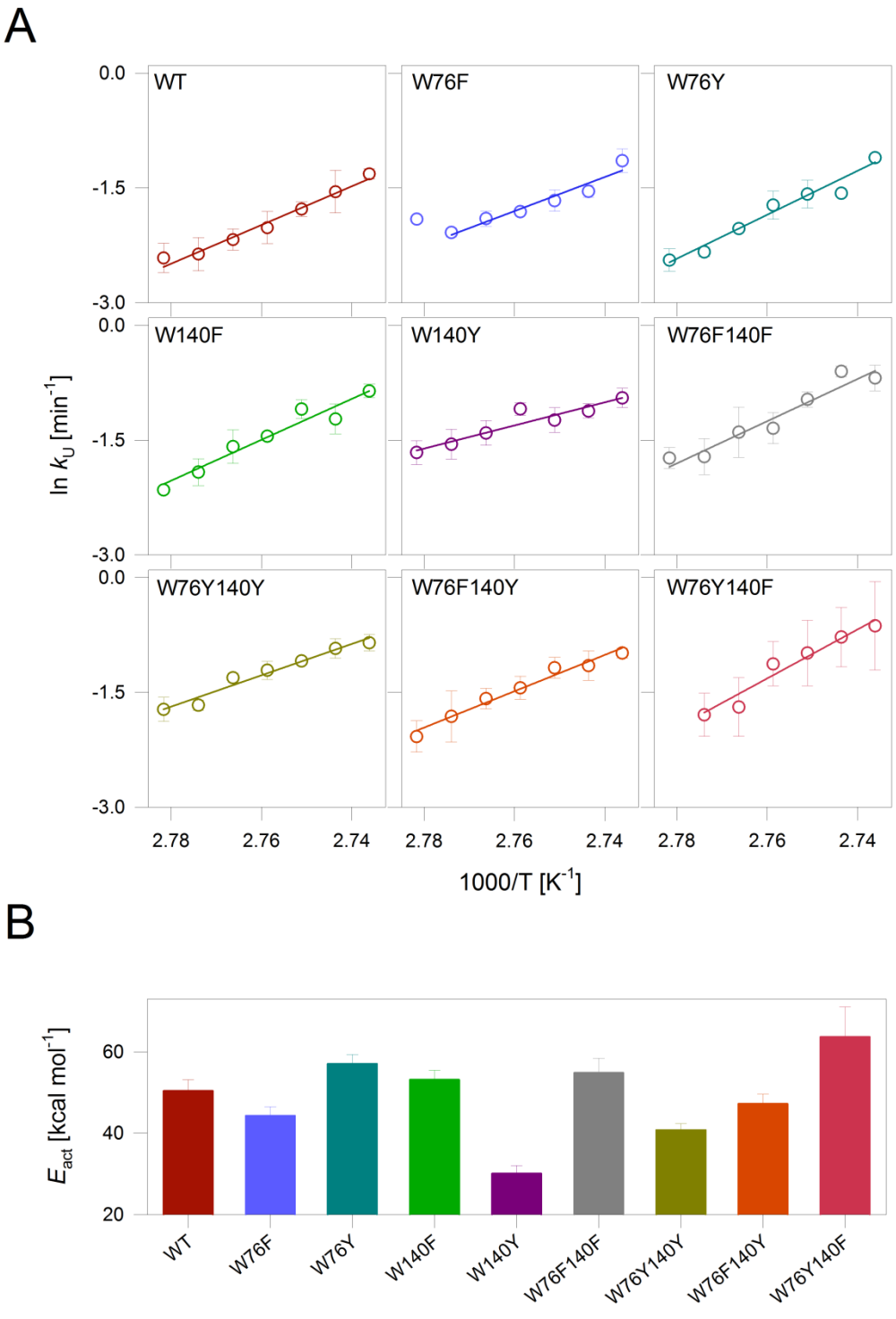

Figure S13. Activation energy calculation from isothermal unfolding kinetics. (A) Arrhenius plots of OmpX and its mutants in 10 mM DPC. Each data point in these plots was generated by fitting the isothermal unfolding profile obtained using CD at 215 nm (shown in Figure S11) to a single exponential function. Unfolding rates were derived at temperatures from 87 °C (as OmpX undergoes thermal denaturation only beyond ~85 °C) to 93 °C (measurements cannot be carried

out at temperatures beyond 95 °C due to limitations of the CD spectropolarimeter) at 1 °C increments. Activation energy (E_{act}) was calculated by fitting the Arrhenius rate plots to a linear function (fits are shown as solid lines). (B) Histograms summarizing the calculated activation energy values for all the mutants. The data shown here is the average value from 3-4 independent experiments and the error bars denote the goodness of fit. Data for each mutant is arbitrarily colored as: WT: maroon; W76F: blue; W76Y: teal; W140F: green; W140Y: purple; W76F140F: grey; W76Y140Y: olive; W76F140Y: orange; W76Y140F: dark pink.

SUPPORTING REFERENCES

[1] S.R. Maurya, D. Chaturvedi, R. Mahalakshmi, Modulating lipid dynamics and membrane fluidity to drive rapid folding of a transmembrane barrel, Sci. Rep., 3 (2013) 1989. DOI: 10.1038/srep01989.

[2] D. Chaturvedi, R. Mahalakshmi, Juxtamembrane tryptophans have distinct roles in defining the OmpX barrel-micelle boundary and facilitating protein-micelle association, FEBS Lett., 588 (2014) 4464-4471. DOI: 10.1016/j.febslet.2014.10.017.

[3] D. Chaturvedi, R. Mahalakshmi, Methionine mutations of outer membrane protein X influence structural stability and beta-barrel unfolding, PLoS One, 8 (2013) e79351. DOI: 10.1371/journal.pone.0079351.

[4] C.P. Moon, K.G. Fleming, Using tryptophan fluorescence to measure the stability of membrane proteins folded in liposomes, Methods Enzymol., 492 (2011) 189-211. DOI: 10.1016/B978-0-12-381268-1.00018-5.

[5] G.H. Huysmans, S.A. Baldwin, D.J. Brockwell, S.E. Radford, The transition state for folding of an outer membrane protein, Proc. Natl. Acad. Sci. U. S. A., 107 (2010) 4099-4104. DOI: 10.1073/pnas.0911904107.

[6] V.R. Agashe, J.B. Udgaonkar, Thermodynamics of denaturation of barstar: evidence for cold denaturation and evaluation of the interaction with guanidine hydrochloride, Biochemistry, 34 (1995) 3286-3299. DOI: 10.1021/bi00010a019.

[7] S.R. Maurya, R. Mahalakshmi, Influence of protein-micelle ratios and cysteine residues on the kinetic stability and unfolding rates of human mitochondrial VDAC-2, PLoS One, 9 (2014) e87701. DOI: 10.1371/journal.pone.0087701.

[8] N.K. Burgess, T.P. Dao, A.M. Stanley, K.G. Fleming, Beta-barrel proteins that reside in the Escherichia coli outer membrane in vivo demonstrate varied folding behavior in vitro, J. Biol. Chem., 283 (2008) 26748-26758. DOI: 10.1074/jbc.M802754200.

[9] D. Gessmann, Y.H. Chung, E.J. Danoff, A.M. Plummer, C.W. Sandlin, N.R. Zaccai, K.G. Fleming, Outer membrane beta-barrel protein folding is physically controlled by periplasmic lipid head groups and BamA, Proc. Natl. Acad. Sci. U. S. A., 111 (2014) 5878-5883. DOI: 10.1073/pnas.1322473111.

[10] C.P. Moon, K.G. Fleming, Side-chain hydrophobicity scale derived from transmembrane protein folding into lipid bilayers, Proc. Natl. Acad. Sci. U. S. A., 108 (2011) 10174-10177. DOI: 10.1073/pnas.1103979108.

[11] J. Reed, T.A. Reed, A set of constructed type spectra for the practical estimation of peptide secondary structure from circular dichroism, Analytical Biochemistry, 254 (1997) 36-40. DOI: 10.1006/abio.1997.2355.